Chapter 7

HYDROPYROLYSIS

Heating coal in hydrogen rather than in an inert gas results in a significantly different product distribution and merits separate consideration. In particular, the increased production of single ring aromatics makes hydropyrolysis a potentially attractive route to chemicals from coal. The changes in the network of thermal reactions engendered by the presence of hydrogen can be roughly classified as follows:

(i) During the early stages of pyrolysis, characterized by rapid tar release, hydrogen penetrates the coal particle and reacts with various free radicals in the gas phase or the condensed phase resulting in increased volatiles production.

(ii) The tar vapors react with hydrogen outside of the particles producing aromatic compounds of smaller molecular weight and, eventually, methane. These reactions include the degradation of condensed rings to single rings and the elimination of phenolic hydroxyl and alkyl substituents.

(iii) After the prolific formation of tar and gases has ceased, hydrogen reacts with active sites on the residual char to produce methane. Initially rapid, this reaction slows down considerably as the char is thermally deactivated.

Processes (ii) and (iii) correspond to what is normally called *hydropyrolysis* or *flash hydrogenation* or *hydrocarbonization*. Sometimes (e.g. ref. 69) a distinction is made between hydropyrolysis, referring to relatively high temperatures (600-1000^{o}C) and short residence times, and hydrocarbonization referring to lower temperatures (450-600^{o}C) and correspondingly longer residence times. Reactions (iii), on the other hand, are characterized by the term *hydrogasification* because they lead to a single product, methane.

In this chapter we will be concerned with hydropyrolysis, i.e. reaction groups (i) and (ii) at the exclusion of hydrogasification which is more properly discussed in the context of coal gasification. In sections 7.1-7.4 we examine four types of experimental systems for hydropyrolysis, the captive sample system, the packed bed system, the modified captive sample system, and the entrained flow system. Section 7.5 contains a review of model compound studies that relate mechanistically to coal hydropyrolysis. The final section 7.6 reviews kinetic modeling of hydropyrolysis.

7.1 CAPTIVE SAMPLE EXPERIMENTS

The apparatus and procedure used in these experiments are the same as the ones used for straight pyrolysis (Section 4.1.2). In fact, the measurements reviewed below were part of the pyrolysis program carried out by the MIT group. The captive sample technique allows relatively rapid removal of volatiles from the

reaction zone so that reactions in group (ii) are largely suppressed and hydropyrolysis is essentially limited to reaction group (i). This constitutes a limitation of the captive sample technique from the standpoint of process-oriented research, where reactions (ii) are utilized to produce the highly desirable single ring aromatics.

Comparisons between weight loss- or total volatiles - under conditions of pyrolysis and hydropyrolysis have been made by Anthony et al. (ref. 125) and Suuberg (ref. 63). Figures 5.8, 5.9 and 5.13 in Chapter 5 taken from the work of Anthony et al. show the weight loss as a function of temperature, pressure and particle size respectively. In Fig. 5.8, the weight loss under 1 atm He (or N_2), 69 atm He and 69 atm H_2 is the same until about 600°C above which the weight loss under 69 atm H_2 exceeds that under 1 atm He which in turn exeeds the weight loss under 69 atm He. In these experiments the sample was rapidly heated to its final temperature at which it was maintained for 5 to 20s.

Figure 7.1 shows the results that Suuberg obtained for the same bituminous coal using a temperature time history consisting of a sharp pulse (see Section 5.2). The weight loss for all three atmospheres is identical, within experimental error, until a peak temperature of about 750°C. Above this temperature, the

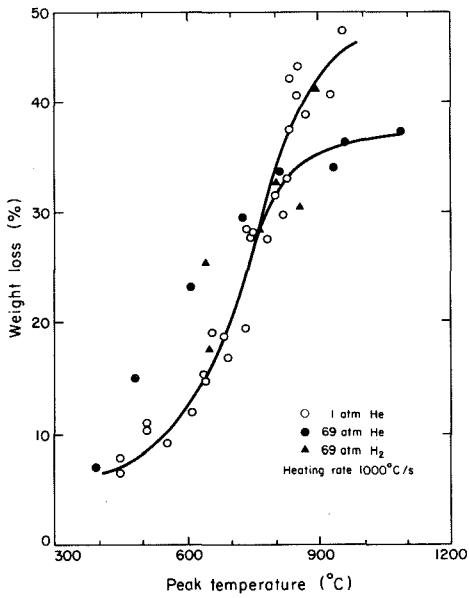

Fig. 7.1. Weight loss vs. peak temperature for pyrolysis and hydropyrolysis of a bituminous coal "Pittsburgh No. 8 (source: ref. 63).

weight loss is essentially the same at 69 atm H_2 and 1 atm He and exceeds that at 69 atm He.

In Figures 5.8 and 7.1, the weight loss curves start diverging at a temperature which marks the transition from conditions free of mass transfer limitations to conditions limited by mass transfer. The different transition temperatures, 600°C in Fig. 5.3 versus 750°C in Fig. 7.1 are evidently due to the different temperature time histories. Increasing the residence time at the highest temperature, lowers the temperature of transition to mass transfer limitations.

Another effect of the prolonged residence time employed in the experiments of Fig. 5.3 is the higher weight loss at 69 atm H_2, compared to that at 1 atm He, a behavior which is not displayed for the pulse-like temperature histories of Fig. 7.1. This result can be attributed to the contribution of hydrogasification reactions (group iii) which is substantial only at the longer residence times. The increased weight loss at the longer residence times due to hydrogasification reactions is also evident in Figs. 5.10 and 5.13.

The most detailed measurements comparing product distributions in pyrolysis and hydropyrolysis were made by Suuberg et al. (refs. 63, 141). Figures 7.2 - 7.4 summarize some of their results.

Figure 7.2 compares the tar yields at 1 atm He, 69 atm He and 69 atm H_2. As we have already seen in Chapter 5 (Fig. 5.11), the yield at 1 and 69 atm He remain the same until 700°C beyond which the yield at 69 atm drops considerably below the atmospheric yield. The yield at 69 atm H_2 is subject to competing effects. On

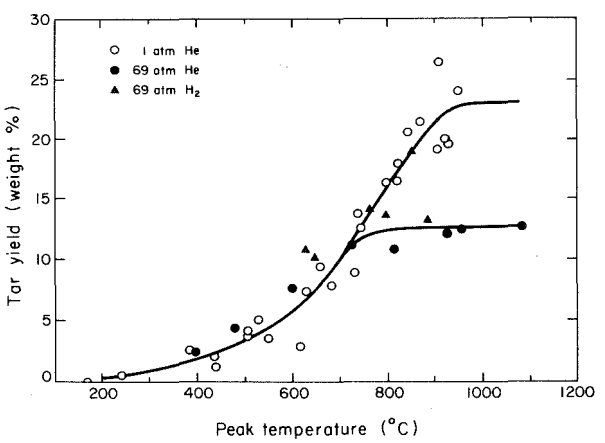

Fig. 7.2. Tar yield vs. peak temperature for pyrolysis and hydropyrolysis of a bituminous coal "Pittsburgh No. 8" (source: ref. 63).

the one hand, hydrogen stabilizes free radicals susceptible to reattachment in the condensed phase. On the other hand, hydrogen reacts with tar precursors in the voids or in the coal melt to produce lower molecular weight products and, at the same time, the increased pressure suppresses the rate of mass transfer away from the particle. The scatter in the data of Fig. 7.2 does not allow quantitative assessment as to the relative magnitude of these effects.

Figure 7.3 compares the yields of methane in 1 atm He and 69 atm H_2. At all temperatures the yield in hydrogen considerably exceeds the yield in the low pressure inert environment. The large differences in the yield are evidently due to the synergism of the two factors mentioned earlier. High pressure reduces the rate of mass transfer and thus increases the probability of secondary reactions including reactions of hydrogenolysis of tar vapors. Additional contributors to the increased methane yield are reaction of molecular hydrogen with active sites in the coal matrix that are not associated with tar precursors. Such reactions include the elimination of methyl substituents on aromatic rings. In connection with Figs. 7.1 - 7.3 it must be noted that the effects of hydrogen on tar and gases are in the opposite direction, whence the more modest effect on total weight loss.

In addition to the bituminous coal, Suuberg studied a lignite with respect to product yields under conditions of pyrolysis and hydropyrolysis (refs. 63, 141). As shown on Fig. 7.4, starting with about 500°C, the methane yield under 69 atm H_2 exceeds the yields under 1 and 69 atm He. The latter two yields remain equal until about 700°C which marks the inception of mass transfer limitations.

Increased yields of hydrocarbon gases other than methane and ethylene were similarly observed in the presence of hydrogen at temperatures as low as 500°C. The low temperature marking the deviation between the gas yields from pyrolysis and hydropyrolysis signifies as before that hydrogen does not only influence the course of secondary reactions of tar precursors but participates in direct reactions with the coal matrix.

In contrast to the yields of other hydrocarbon gases, the yields of ethylene at 1 atm He and 69 atm H_2 were equal and, beginning at 700°C, surpassed the yield at 69 atm He.

Although the amount of tar obtained from lignite was low and, hence, subject to larger measurement error, it could be still observed that the tar yields at 1 atm He and 69 atm H_2 were higher than the yield at 69 atm He. The weight loss at 69 atm H_2 slightly exceeded that at 1 atm He. Compared to the bituminous coal, lignite displays a somewhat different weight loss dependence on total pressure and hydrogen pressure probably due to the difference in the *relative* tar yields between the two coals.

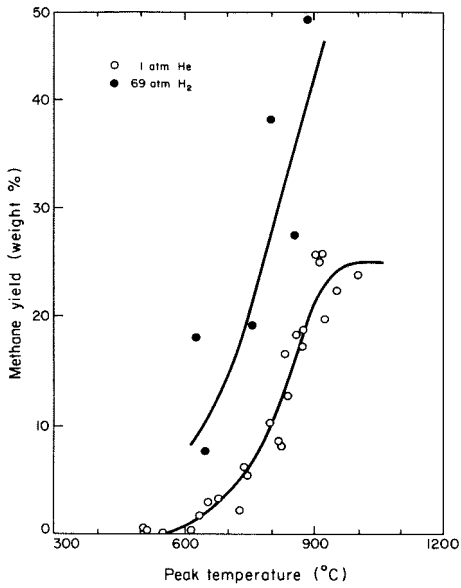

Fig. 7.3. Methane yield vs peak temperature for pyrolysis and hydropyrolysis of a bituminous coal "Pittsburgh No. 8" (source: ref. 63).

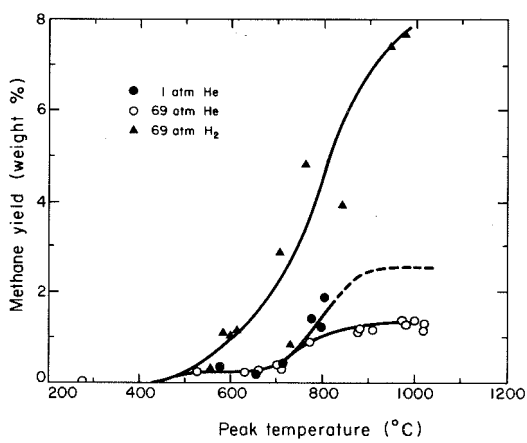

Fig. 7.4. Methane yield vs. peak temperature for pyrolysis and hydropyrolysis of a lignite (source: ref. 63).

7.2 PACKED BED EXPERIMENTS

In this arrangement, the coal sample is held stationary in a section of a tubular reactor, which we shall call the *hydropyrolysis section*, where it is subjected to a temperature program under hydrogen flow. The volatile products carried in the hydrogen stream pass through an additional heated section, which we shall call the *hydrogenolysis section*, and after quenching are conducted to product collection and sampling equipment. By regulating the hydrogen flow rate and suitably controlling the temperatures in the hydropyrolysis and hydrogenolysis sections of the tubular reactor it is possible, in principle, to control the temperature and residence time of the solid and the volatile products independently.

In early experiments by Hiteshue et al. (refs. 142, 143) utilizing the packed bed arrangement, the heating period was relatively long, about three minutes, and the temperatures of the solid sample and the volatile products could not be controlled independently. In a recent study, Finn et al. (ref. 144) used a two-segment tube to implement independent temperature control of solids and volatiles while achieving heating times as short as half a minute.

A schematic of the apparatus used by Finn et al. is shown in Fig. 7.5. Coal was placed in an 8 cm long bed in the hydropyrolysis section and subjected to a

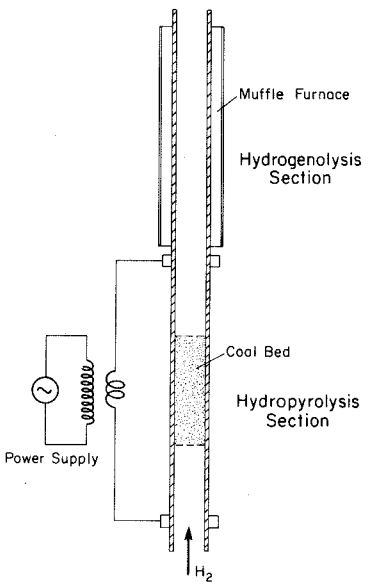

Fig. 7.5. Schematic of two-segment hydropyrolysis reactor used by Finn et al. (ref. 144).

temperature pulse by direct resistive heating of the tube wall using a low voltage transformer. The hydrogenolysis section was maintained at constant temperature by a muffle furnace. The reactor tube was 8 mm ID and the temperature was recorded at the tube wall. One disadvantage of using a massive coal sample was that the true heating period was probably considerably longer than the half minute reported for the tube wall. Another disadvantage was the extensive secondary reactions of tar vapors and other volatiles on the coal surface before entering the second section intended for hydrogenolysis.

Figures 7.6 - 7.9 show some of the results of Finn et al. (ref. 144). The yield of various single ring aromatics vs. peak temperature is shown in Fig. 7.6. The temperature pulse, common in both reactor sections, consisted of a rising segment (heating rate $7^{o}K/s$) immediately followed by rapid cooling (three seconds). The products consisted of approximately equal amounts of benzene-toluene-xylene (BTX) and phenol-cresols-xylenols (PCX). Both classes of products passed through a maximum at a temperature slightly below $1000^{o}K$. The maximum yield of BTX + PCX was about 5 per cent.

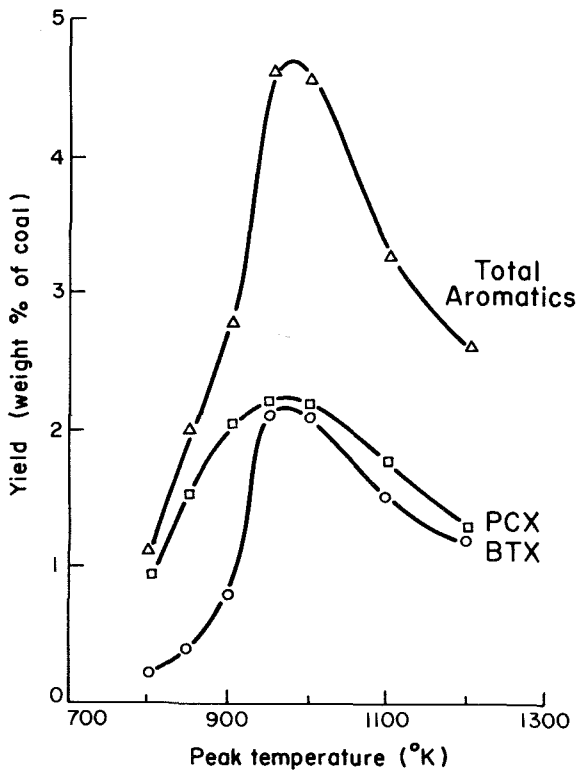

Fig. 7.6. Yield of single ring aromatic products vs. peak temperature for hydropyrolysis of a bituminous coal at 150 bar pressure and 11s hydrogenolysis residence time (source: ref. 144).

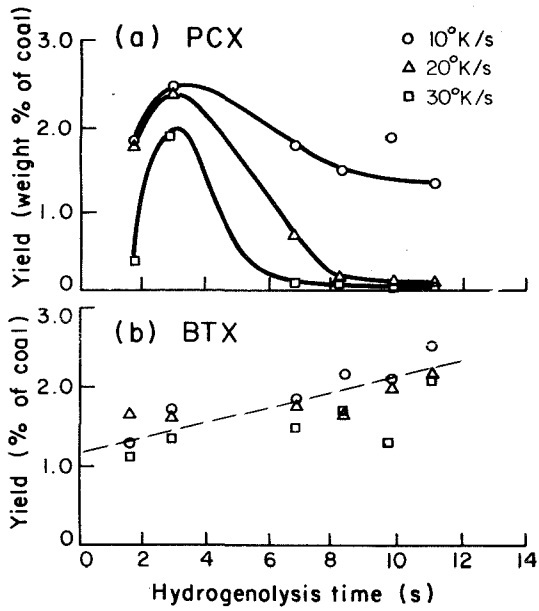

Fig. 7.7. Yield of BTX and PCX vs. hydrogenolysis time at different heating rates for hydropyrolysis of a bituminous coal at 150 bar pressure and 1000°K peak temperature (source: ref. 144).

Fig. 7.7 plots the product yields obtained under the same type of temperature pulse as in Fig. 7.6 but for different heating rates and hydrogenolysis times. The yield of BTX increases steadily with hydrogenolysis time and is rather insensitive to heating rate. These trends can be explained by the fact that BTX is an intermediate product resulting from the degradation of tar and in turn being converted to methane. Since the latter reaction is slower, the maximum of BTX corresponds to hydrogenolysis times larger than ten seconds and is not shown in the figure. The effect of heating rate is smaller and largely masked by the scatter in the data.

In contrast to the yield of BTX, the yield of PCX shows some rather striking trends. At fixed heating rate, the yield passes through a maximum at about three seconds hydrogenolysis time. The presence of this maximum suggests consecutive reactions from tars to PCX and PCX to BTX or directly to methane. Since the decrease in PCX is not accompanied by a commensurate increase in BTX, the direct conversion of PCX to methane seems to be the predominant route. At fixed

hydrogenolysis time, PCX decreases rather rapidly with increasing heating rate probably due to the shorter *solids* exposure to high temperatures decreasing the yield of precursor tar vapors. Why this same effect is not shown by the yield of BTX remains a vexing question.

A different temperature-time program was used in the measurements reported in Figs. 7.8, 7.9. After rising to its maximum value, the temperature in the hydropyrolysis section was maintained constant for ten to fifteen minutes while the temperature in the hydrogenolysis section was kept at some other constant value throughout the run Figure 7.8 shows various product yields vs. hydrogenolysis temperature. Since the hydrogen flux was kept constant in these runs, variation of the hydrogenolysis temperature was accompanied by variation of the hydrogenolysis time. Nevertheless, the yield curves still reflect the fact that tar vapors are precursors for benzene and other light aromatics which in turn are converted to the final product methane. Figure 7.9 plots the yields of several products vs. hydropyrolysis temperature. The maximum yield of benzene, about 12 percent, is quite promising from the standpoint of producing chemicals from coal.

7.3 MODIFIED CAPTIVE SAMPLE EXPERIMENTS

To achieve high heating rates and prevent secondary reactions on the coal particle surface, Graff et al. (refs. 145, 146) developed an experimental technique

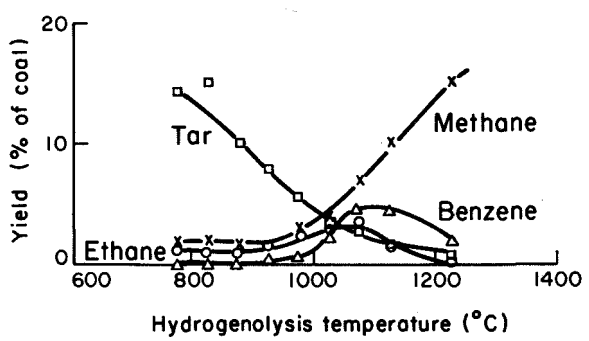

Fig. 7.8. Product yields vs. hydrogenolysis temperature for a bituminous coal at heating rate $1^{o}K/s$, peak hydropyrolysis temperature $750^{o}K$ and hydrogen pressure 100 bar (source: ref. 144).

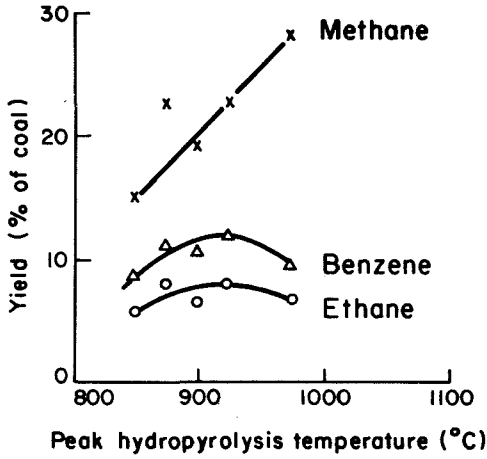

Fig. 7.9. Product yields vs. peak hydropyrolysis temperature for a bituminous coal at heating rate $5^{o}K/s$, hydrogenolysis temperature $1123^{o}K$ and hydrogen pressure 150 bar (source: ref. 144).

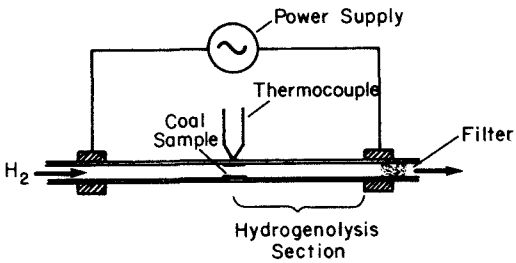

Fig. 7.10. Modified captive sample reactor for coal hydropyrolysis (source: ref. 145).

combining the advantages of the captive sample and the packed bed techniques. The reaction section of their setup is shown in Fig. 7.10. The reactor consists of a stainless steel tube 5.1 mm ID, 6.3 mm OD and 30 cm length capable of withstanding up to $1000^{o}C$ temperature and 100 atm pressure. The finely ground coal is deposited on a circular region in the middle of the tube. The whole reactor tube is heated resistively by means of a DC power supply switched on and off by a control circuit. As with the captive sample equiment described in Chapter 4, resistive heating is applied at two levels. The first and higher level serves to heat the tube to the preset temperature at a rate up to $1500^{o}C/s$. After the desired temperature is established, a control circuit switches power to the lower

level, adequate to maintain the tube at the desired steady temperature for the duration of the experiment. A spot welded thermocouple serves to indicate the temperature and activate the switching circuit.

After establishing the hydrogen flow at the desired pressure and flow rate, the power supply is switched on and the volatiles released from the coal sample are carried in the hydrogen stream through the downstream section of the tube which constitutes the section for hydrogenolysis. While this experimental setup provides identical hydropyrolysis and hydrogenolysis temperatures, the sample heating technique can be applied in conjunction with a two-segment reactor with separate control of the hydrogenolysis temperature. The residence time in the hydrogenolysis section is in all cases controlled by the hydrogen mass flow rate, with due allowance for the volumetric expansion at the reaction temperature.

The reaction products are collected in evacuated tanks from which samples are drawn for analysis by gas chromatography. An ingenious technique is used to prevent undue dilution by hydrogen of the product gas. A thermal conductivity cell detects the level of products in the product stream and only when this level is above a preset value is the product stream directed to the sample tanks. The residual char is determined by oxidation in place and analysis of the carbon oxides produced. Heavy liquids not detectable by gas chromatography, are reported as "carbon deficit."

Some of the results reported by Graff et al. (refs. 145, 146) for a high volatile bituminous coal (Illinois No. 6) are reproduced in Figs. 7.11, 7.12 with the yields expressed as carbon in the products as a percentage of carbon in the coal. Figure 7.11 shows the yields of methane, ethane and propane vs. reaction temperature for fixed solids and vapors residence time. The monotonically increasing yield of methane is obviously due to the fact that this gas is the final hydrogenolysis product of tar vapors and hydrocarbon gases. Ethane, on the other hand as an intermediate product passes through a maximum. The monotonic decrease of propane might be due to the decomposition of its precursor propyl radicals to ethylene and methyl radicals, favored at the higher temperatures.

Figure 7.12 plots the yields of BTX and tar versus reaction temperature. The tar was determined indirectly as the difference between the original carbon and the carbon in all measured products, including char. The determination by difference is obviously subject to considerable error. As in the studies discussed in Section 7.2, the yield of BTX passes through a maximum of about 12 percent. This yield is comparable to that shown in Fig. 7.8 corresponding to much lower heating rates. The temperature of the maximum was in both cases about 800^{o}C. The similarity of the results in Figs. 7.8 and 7.12 indicates that, isolated from other operating variables, heating rate has a relatively minor effect on product yields.

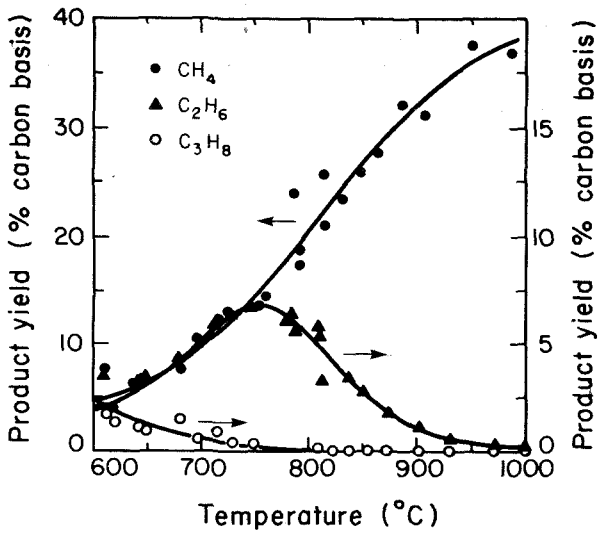

Fig. 7.11 Yield of gaseous hydrocarbons vs. temperature for hydropyrolysis of a bituminous coal "Illinois No. 6" at 100 atm H_2 and 0.6s hydrogenolysis time (source: ref. 146).

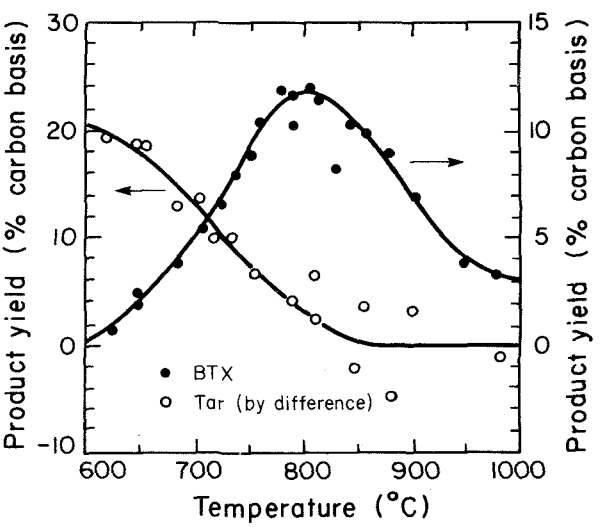

Fig. 7.12. Yields of BTX and tar (by difference) vs. temperature for hydropyrolysis of a bituminous coal "Illinois No. 6" at 100 atm H_2, 650°C/s heating rate and 0.6s hydrogenolysis time (source: ref. 146).

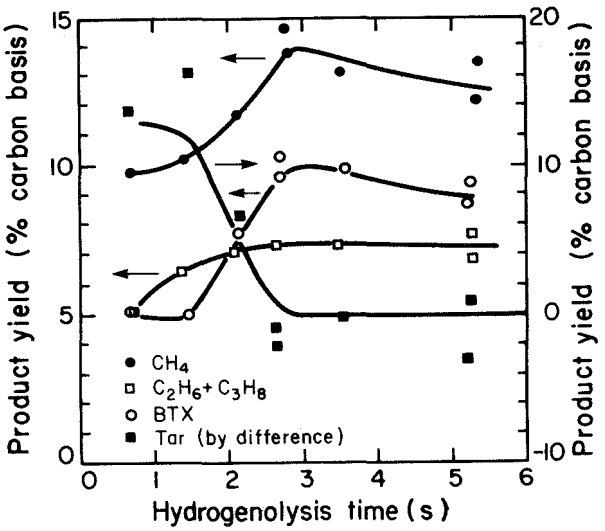

Fig. 7.13. Product yields vs. hydrogenolysis time for hydropyrolysis of a bituminous coal "Illinois No. 6" at 700°C, 100 atm H_2 and 650°C/s heating time (source: ref. 146).

Figure 7.13 shows the dependence of product yields on hydrogenolysis time (volatiles residence time) at 700°C. The maximum in the BTX yield is attained at about three seconds. This optimal time would decrease to a fraction of a second at 800°C as inferred from the previous figure. The shallow maximum in the yield of methane is somewhat puzzling in view of the slow decline of BTX at times larger than three seconds.

7.4 ENTRAINED FLOW EXPERIMENTS

While the modified captive sample reactor is well suited to fundamental kinetic studies, the entrained flow reactor is better suited to process development by being amenable to scale-up to pilot plant units. Entrained flow experiments are difficult to interpret kinetically because coal particles react continuously during their passage through the reactor, therefore, the volatile products have a distribution of residence times for hydrogenolysis. On the other hand, the entrained flow reactor operating at steady state generates large samples suitable for the accurate measurement of product yields. An entrained flow reactor for hydropyrolysis generally has geometry similar to an entrained flow pyrolysis reactor, but must be capable of operating at high pressures.

An entrained flow system was used by Fallon et al. (ref. 147) to study the hydropyrolysis of a lignite and a subbituminous coal at 700-900°C and 500-1,500 psia of hydrogen. The products up to and including BTX were determined by gas chromatography while the heavier liquids were collected and analyzed at the end

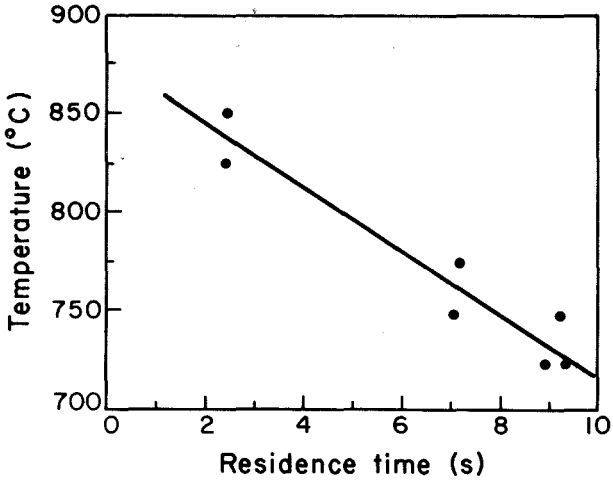

Fig. 7.14. Locus of maximum BTX yield for hydropyrolysis of lignite at 2500 psia H_2 (source: ref. 147).

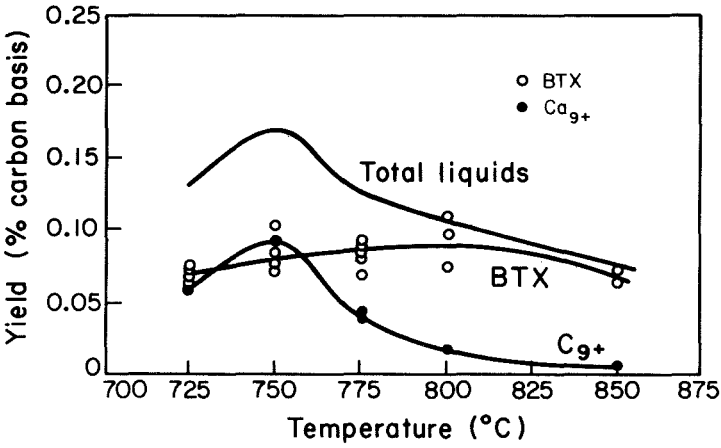

Fig. 7.15. Maximum yields of BTX and C_{9+} liquids vs. temperature for hydropyrolysis of lignite at 2000 psia H_2 (source: ref. 147).

of each experiment. Several runs with lignite explored the effect of the three principal variables on the yield of products, especially BTX. At fixed residence time and pressure, the yield of BTX passes through a maximum in the range 700-800°C. Likewise, at fixed temperature and pressure, the yield of BTX becomes maximum at some intermediate residence time, past which it declines rapidly to

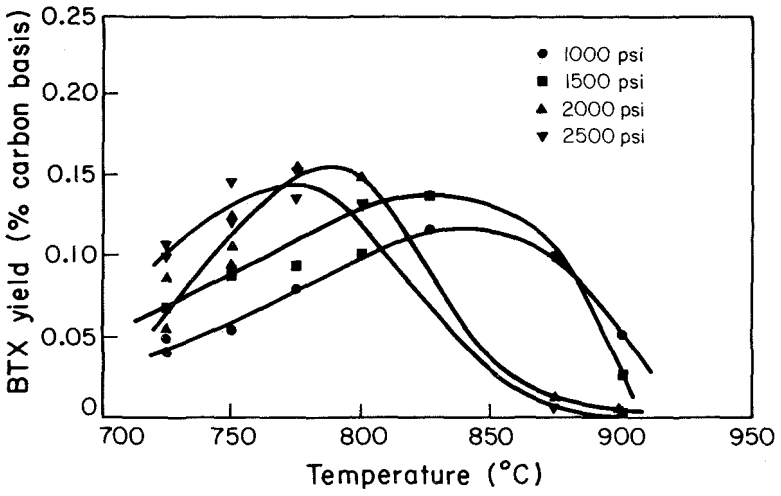

Fig. 7.16. Maximum BTX yield vs. temperature for hydropyrolysis of a subbituminous coal at various hydrogen pressures (source: ref. 147).

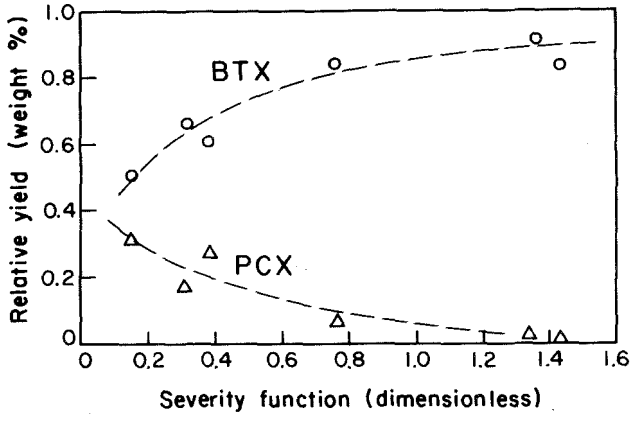

Fig. 7.17. Relative yields of BTX and PCX in the liquid products as a function of severity for the hydropyrolysis of a lignite at 2000 psia H_2 (source: ref. 148).

zero. On the other hand, at fixed residence time, the yield vs. temperature curve is rather broad around the maximum value. The maximum yields under most conditions were in the range 8-10 percent in terms of carbon conversion. Figure 7.14 is a locus of temperature-residence time conditions under which the BTX yield was near its maximum value of 8-10 percent. The maximum yields are shown in Fig. 7.14

to increase as the hydrogen pressure increased from 500 to 2000 psia. Upon further increasing the pressure to 2500 psia, the maximum yield remained essentially unchanged but the residence time required to attain this yield decreased.

Liquids heavier than BTX (C_{9+}) were also observed in significant yields as shown in Fig. 7.15. These liquids were much lighter than pyrolysis tars consisting of about 40 percent naphthalene and only trace amounts of phenols. However, being considerably more reactive than BTX, they readily declined with increasing temperature.

Hydropyrolysis experiments performed using a subbituminous coal resulted in BTX yields as high as 15 percent compared to the 10 percent obtained with lignite. Figure 7.16 shows the maximized yield of BTX (with respect to residence time) as a function of temperature at four pressure levels.

In another recent study, Beeson et al. (ref. 148) studied the hydropyrolysis of a lignite using an entrained flow reactor with controlled axial temperature profiles. Although the intent was to determine the effect of the heating rate, the ability to vary the axial temperature profile offers a potentially useful variable for product optimization.

The results reported are particularly interesting relative to the detailed breakdown of liquids in the gasoline boiling range into several fractions: BTX, C_{9+} aromatics, indenes + indans, phenols + cresols and naphthalene. Overall yields of these liquid products (carbon in the liquids as a fraction of carbon in the original coal) ranged between 0.07 and 0.15. The mass fraction of phenols and cresols in the liquids was as high as 0.76 indicating that the phenolic compounds constitute the primary hydropyrolysis products from lignite. The phenolic products react further to BTX and methane at a rate depending on temperature and hydrogen pressure.

Figure 7.17 shows the variation of the relative yields of BTX and phenol + cresol as a function of a severity parameter defined by

$$\text{severity} = \int_0^t k_0 \, dt$$

where $k_0 = 9 \times 10^5 \exp(-30{,}700/RT)$. The rate constant k_0 was assigned by reference to some earlier data on anthracene hydrogasification, therefore, the severity parameter is a somewhat arbitrary measure of the combined effect of temperature and residence time.

Two other related hydropyrolysis programs with emphasis on process and hardware development are the Cities Service short residence time hydropyrolysis program (ref. 149) and the Rockedyne program (ref. 150). The City Service program has employed a laboratory scale entrained flow reactor (about 1 Kg coal/hr) while the Rockedyne program has utilized a process development entrained flow reactor (about 200 Kg coal/hr). The distinguishing feature of the second reactor is the

rapid mixing between feed coal and hydrogen, achieved by a "rocket engine" injector. Results reported to date for a lignite showed maximum BTX yields of about 10 percent (City Service) or total liquid yields of about 30-40 percent (Rockedyne).

7.5 MODEL COMPOUND STUDIES

As mentioned at the beginning of the chapter, hydropyrolysis reactions include (i) reactions of hydrogen with the condensed phase during the stage of liquids formation (ii) hydrogenolysis of the vapors in the gas phase to produce PCX (phenols), BTX and light hydrocarbon gases. The model compound studies discussed below are useful primarily in understanding the mechanism and kinetics of hydropyrolysis reactions in class (ii) which we have earlier labelled as hydrogenolysis. Some general issues that are of particular interest are the mechanisms of degradation of ring systems, e.g. naphthalene to toluene or benzene to methane; and the mechanisms of dealkylation and dehydroxylation, e.g. toluene to benzene or cresol to toluene. In addition to reaction pathways and mechanisms, it would be valuable to possess a reasonable kinetic description of the effect of operating variables on product yields.

Virk et al. (ref. 151) analyzed existing data on unsubstituted aromatic hydrocarbons and found that the rates of disappearance of each compound in pyrolysis and hydrogenolysis were roughly equal, although the products were different. In the absence of hydrogen, successive condensation and dehydrogenation led to a final solid product, coke. In the presence of hydrogen, the final product was methane. Intermediate products with a smaller number of fused rings were not specifically identified. Based on the approximate equality of the rates of pyrolysis and hydrogenolysis they proposed that both reactions have a common rate determining step, namely the "destabilization" of the aromatic ring. Although the mechanism of this step was not identified, its rate was assumed to be related to the ring delocalization energy.

Penninger and Slotboom (ref. 152) reviewed experimental data on the hydrogenolysis of several substituted and unsubstituted aromatics. For the case of unsubstituted naphthalene and phenanthrene they concluded that ring cracking occurs through the formation of an intermediate hydroaromatic compound. For example, naphthalene is first hydrogenated to tetralin which subsequently decomposes to various alkylbenzenes. The mechanism of the crucial first step, the hydrogenation of the unsubstituted aromatic, was not identified. On the other hand, the subsequent hydrogenolysis of the hydroaromatics was explained by free radical mechanisms.

The hydrogenolysis of hydroaromatics can be illustrated with the reactions of tetralin which have already been discussed in a different context (Section 6.3.2). We are here interested in the mechanism of utilization of molecular hydrogen. One possibility is offered by the reaction

$R\cdot + H_2 \rightleftarrows H\cdot + RH$

where R· is a carbon centered radical, more specifically an alpha radical. Despite the unfavorable equilibrium (ΔG is about 18,800 at $300^{o}K$), this reaction increases the concentration of hydrogen atoms which can then participate in addition reactions such as

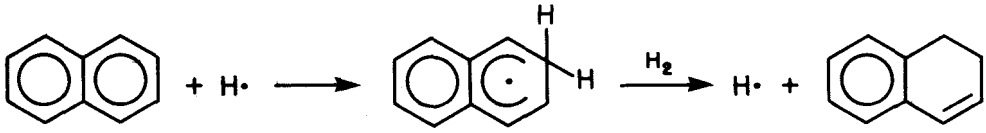

The dihydronaphthalene produced can be subsequently hydrogenated to naphthalene by the same mechanism, via the addition of a hydrogen atom. No mechanism has so far been proposed for the direct (pericyclic) addition of molecular hydrogen, although the possibility cannot be excluded.

Increased concentration of hydrogen atoms due to the presence of molecular hydrogen is effective in tetralin decomposition via addition and opening of the saturated ring (Section 6.3.2) and in dealkylation. The latter reaction may be illustrated by the example

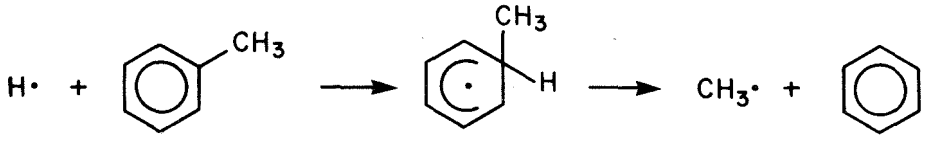

with the methyl radical ending up as methane after hydrogen abstraction.

Cypres and Bettens (refs. 47-49) studied the pyrolysis of phenol and cresols in the absence of hydrogen and proposed non-free-radical mechanisms for these reactions (see Section 3.7). The mechanisms proposed leave some open questions and cannot be readily extended to include the effect of molecular hydrogen.

7.6 MODELING

We start by recalling the classification of reactions into groups (i)-(iii) defined at the beginning of the chapter. Most of the models concerning hydrogen-coal reactions have been addressed to reaction group (iii) in the context of coal gasification to methane. Models of this type will not be discussed here since they are not relevant to the early phases of hydropyrolysis. Reaction groups (i) and (ii), dominating the early phases of hydropyrolysis, have been considered in only a few modeling studies, three of which are discussed below.

The experimental work of Anthony et al. (refs. 125, 126) and Suuberg et al. (refs. 63, 141) have demonstrated the effects of inert pressure, hydrogen pressure and particle size on the total yield of volatiles (see e.g. Figs. 5.4, 5.9, 7.1). To quantitatively describe such effects which are intimately related to mass transfer limitations Anthony et al. (ref. 125) proposed the following set of phenomenological reactions

$$\text{coal} \rightarrow \nu_1 V^* + \nu_2 V + S^* \tag{7.1}$$

$$V^* + H_2 \rightarrow V \tag{7.2}$$

$$V^* \rightarrow S \tag{7.3}$$

$$S^* + H_2 \rightarrow V + S^* \tag{7.4}$$

$$S^* \rightarrow S \tag{7.5}$$

Coal decomposes to "unreactive" volatiles V, reactive volatiles V^* and a reactive solid S^*. The unreactive volatiles consist of gases such as methane, steam, carbon oxides, light liquids (e.g. BTX) and heavier products, tar. The reactive volatiles presumably consist of free radicals or other unstable molecules. S^* is a reactive solid susceptible to hydrogenation by the fourth reaction while S is a solid which participates in no further reactions in the time scale of interest.

Mass transfer enters in the problem through a balance for species V^* in the voids of the coal particle. Assuming steady state conditions, the mass balance becomes

$$K(c^* - c_\infty^*) = \nu_1 r_1 - r_2 - r_3 \tag{7.6}$$

where c^*, c_∞^* are the concentrations of V^* inside and outside the particle, r_1, r_2,... are the rates of reactions (7.1), (7.2),...., and K is a mass transfer coefficient. The reaction rates were expressed in first or second order form and the rate constants were specified numerically to match the experimental data (ref. 125). From our standpoint it is important to take notice of the fundamental assumptions or approximations of the model which were (i) the gas space inside the particle has fixed volume and uniform composition (ii) the concentration of hydrogen inside the particle is uniform and equal to the outside concentration (iii) all reactive species can be lumped into one, V^* (iv) the mass transfer coefficient is inversely proportional to the pressure but independent of particle size. The yield of total volatiles calculated on the basis of this model was in most respects in good agreement with the experimental yield. However, the model predicted a stronger pressure dependence than experimentally observed while it failed to predict the observed effect of particle size in the presence of hydrogen. Both points of disagreement seem to derive from assumption (ii) and to

suggest the existence of a hydrogen pressure drop from the outside to the inside of the particle.

In a relatively recent study (ref. 135), Russel et al. carried out an elegant and comprehensive theoretical analysis of hydropyrolysis reactions coupled with intraparticle mass transfer. They employed a reaction system identical to (7.1)-(7.5) except that reaction (7.2) was assumed instantaneous, therefore V^* and H_2 disappeared on a reaction front gradually progressing towards the center of the particle. Mass transfer was described by the "dusty gas" model, taking into account fluxes due to diffusion and pressure gradients. For this purpose the coal particle was assumed to possess a stable pore structure, an assumption which applies reasonably well to nonsoftening coals but not to sofening coals (see Chapter 5). The model was nonetheless tested against the pyrolysis and hydropyrolysis data from a high volatile bituminous coal (refs. 125, 126).

Recent hydropyrolysis modeling work by the MIT group was presented by Schaub et al. (ref. 153). Although this publication gives very few details, the two basic premises of the analysis can be summarized as follows:

(i) The hydropyrolysis reactions are represented by the scheme below where M is the familiar by now metaplast (Chapter 5), S is a reactive solid termed "semi-coke" and A is another reactive intermediate in the condensed phase. Step 3 is the transport of metaplast molecules from the coal melt to the gas phase as tar. All other steps are chemical in nature.

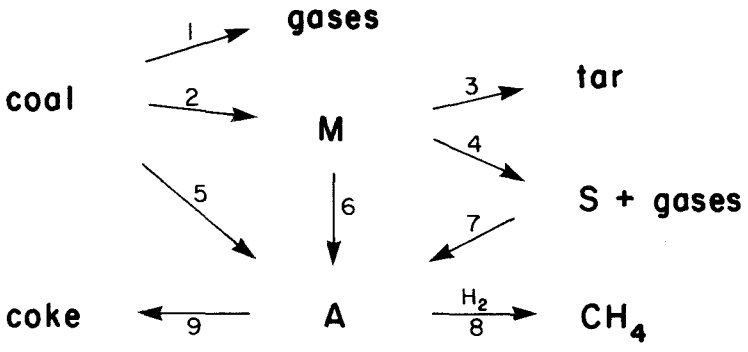

(ii) Step 8 requires the diffusion of hydrogen in the condensed phase which is initially a melt but later becomes a solid, char.

The reaction scheme shown above differs considerably from the one utilized in refs. 125, 135. It employs a more complex network of consecutive reactions and differentiates between three products, gases, methane and tar. It also assumes that hydrogen reacts with a species in the condensed phase rather than the gas phase and predicts that the tar yield depends on total pressure but not on the

nature of the surrounding gas. Unfortunately, the limited experimental data available (Fig. 7.2) are insufficient to test this crucial prediction. Another noteworthy feature of the model is the consideration of hydrogen diffusion through the coal melt, enhanced by the stirring action of the evolving bubbles. Although some of its detailed assumptions could be questioned, this model represents the most physically realistic effort in hydropyrolysis modeling.